



Published in final edited form as:

*Nat Immunol.* 2015 April ; 16(4): 406–414. doi:10.1038/ni.3108.

## Proinflammatory microenvironments within the intestine regulate differentiation of tissue-resident CD8 T cells responding to infection

Tessa Bergsbaken<sup>1</sup> and Michael J. Bevan<sup>1,\*</sup>

<sup>1</sup>Department of Immunology and Howard Hughes Medical Institute, University of Washington, Seattle, WA 98109, USA

### Abstract

We report that oral infection with *Yersinia pseudotuberculosis* (Yptb) results in development of two distinct populations of pathogen-specific CD8 tissue-resident memory T ( $T_{RM}$ ) cells in the lamina propria (LP). CD103<sup>-</sup> T cells did not require transforming-growth factor- $\beta$  (TGF- $\beta$ ) signaling, but were true resident memory cells. Unlike CD103<sup>+</sup> CD8 T cells, which were TGF- $\beta$ -dependent and scattered in the tissue, CD103<sup>-</sup> T cells clustered with CD4 T cells and CX3CR1<sup>+</sup> macrophages and/or dendritic cells around areas of bacterial infection. CXCR3-dependent recruitment to inflamed areas was critical for development of the CD103<sup>-</sup> population and pathogen clearance. These studies have identified the preferential development of CD103<sup>-</sup> LP  $T_{RM}$  cells in inflammatory microenvironments within the LP and suggest that this subset plays a critical role in controlling infection.

Effector CD8 T cells generated during infection with bacterial or viral pathogens undergo an activation phase that allows their entry into a variety of peripheral tissues, including the intestine<sup>1</sup>. During this window, surface expression of the integrin  $\alpha_4\beta_7$  and chemokine receptor CCR9 facilitate CD8 T cell entry into the intestinal tissue<sup>2-4</sup>. Once they enter the tissue, CD8 T cells acquire a tissue-resident memory ( $T_{RM}$ ) phenotype characterized by expression of CD69, the integrin CD103, and enhanced effector function including constitutive expression of granzyme B<sup>5,6</sup>. Intestinal CD8  $T_{RM}$  cells are not able to re-enter the circulation<sup>4</sup>, and their long-term maintenance within the tissue provides immediate local protection against subsequent infection<sup>7</sup>.  $T_{RM}$  cells have a unique transcriptional profile when compared to other memory T cell subsets, and data suggests a core transcriptional program defines  $T_{RM}$  cells from disparate tissues<sup>8,9</sup>; however, tissue- and pathogen-specific features could also regulate the phenotype and function of  $T_{RM}$  cells.

Users may view, print, copy, and download text and data-mine the content in such documents, for the purposes of academic research, subject always to the full Conditions of use:[http://www.nature.com/authors/editorial\\_policies/license.html#terms](http://www.nature.com/authors/editorial_policies/license.html#terms)

\*Correspondence: mbevan@uw.edu.

Author contributions

TB and MJB designed experiments and wrote the manuscript, TB performed experiments and analyzed data.

COMPETING FINANCIAL INTERESTS

The authors declare no competing financial interests.

We are only beginning to understand the signals within the intestinal tissue that dictate development of  $T_{RM}$  cells, particularly in the context of local infection. CD8 T cells traffic to the intestine and persist after infections that have limited intestinal involvement<sup>1</sup>. However, evidence suggests that intestinal CD8  $T_{RM}$  cells that develop in the absence of local infection have reduced CD69 and CD103 expression when compared to those generated during local tissue colonization<sup>7</sup>, suggesting signals received during local infection lead to unique or more effective populations of  $T_{RM}$  cells. Development of the intestinal  $T_{RM}$  population is influenced by the local cytokine environment; transforming growth factor- $\beta$  (TGF- $\beta$ ) is ubiquitously expressed in the intestine and critical for the formation of  $T_{RM}$  cells in response to both local and systemic infection<sup>7,10,11</sup>. Inflammatory signals induced during intestinal infection may also influence  $T_{RM}$  cell development, and culture of effector CD8 cells *ex vivo* suggests several inflammatory cytokines potentially influence markers of tissue residence<sup>10,12</sup>. The presence of antigen in the intestinal tissue is not required for the development of CD8  $T_{RM}$  cells<sup>10</sup>, but it is not known whether antigen-dependent signals affect the phenotype of  $T_{RM}$  populations in the context of tissue-specific infection.

*Yersinia pseudotuberculosis* (Yptb) is a gram negative bacterial pathogen that causes disease characterized by gastroenteritis, and mesenteric lymphadenitis, and may spread to the liver and spleen and cause fatal disease. CD8 T cells responding to Yptb infection are a critical component of protection from subsequent challenge<sup>13-15</sup>. Yptb is able to colonize the intestinal tissue and stimulate a robust antigen specific CD8 T cell response; however, the CD8 T cell response to this oral pathogen in the intestinal tissue has not been characterized. Yptb and other intestinal pathogens can spread to systemic organs directly from the intestine and do not rely on creating a bacterial pool in Peyer's patches and mesenteric lymph nodes to access the bloodstream<sup>16,17</sup>; therefore, directing an anti-microbial CD8 T cell response to local areas of infection in the intestinal wall may be critical for controlling bacterial dissemination and clearance.

Here we have utilized Yptb infection via the natural route as a model to study the CD8 T cell response to a pathogen that causes robust intestinal disease. The data indicate Yptb induces a strong intestinal CD8 T cell response and results in the development of a heterogeneous population of intestinal CD8  $T_{RM}$  cells. A portion of antigen-specific CD8 T cells are dependent on signals via the TGF- $\beta$  receptor (TGF- $\beta$ R), express CD103 and are evenly distributed throughout the intestinal epithelium and LP. The remainder are CD103<sup>-</sup>, originally clustered around areas of Yptb infection in the LP, where they control bacterial replication. The CD103<sup>-</sup> LP CD8s are developmentally distinct from their CD103<sup>+</sup> counterparts, as they do not require TGF- $\beta$ R signaling but instead require access to areas of bacterial infection and inflammation for their differentiation. These findings indicate localization of CD8  $T_{RM}$  to distinct microenvironments within the infected intestine regulates both their phenotype and function.

## Results

### *Yersinia* generates a robust intestinal CD8 T cell response

Infection of B6 mice with *Yersinia* species results in a strong CD8 T cell response to a peptide from YopE, an effector protein translocated into the cytosol of infected host cells<sup>14,15</sup>. To develop a more tractable system to allow us to follow antigen specific CD8 T cell responses during intestinal infection, we generated a strain of *Yersinia pseudotuberculosis* expressing the model antigen ovalbumin. Fusion of a fragment of ovalbumin to YopE has been demonstrated to prime OT-I T cells specific for the ovalbumin peptide SIINFEKL<sup>18</sup>. Previous studies have used integration of multiple genes into the *Yersinia* virulence plasmid, but we found a strain constructed in this manner was attenuated during oral infection (data not shown). Therefore, we generated a YopE::OVA fusion construct and replaced the coding sequence of the YopO gene on the pIB1 virulence plasmid of *Yersinia pseudotuberculosis* (Yptb-OVA) (**Supplementary Fig. 1a,b**). Notably, YopO-deficient *Yersinia* strains do not display decreased virulence *in vivo*<sup>19</sup>, and use of the endogenous YopO promoter allows production of physiological amounts of the fusion protein, thus preventing competition with other translocated virulence proteins.

We transferred  $10^4$  naive GFP OT-I T cells into mice and infected them orally with Yptb-OVA. This resulted in expansion of OT-I T cells in the spleen, while infection with a Yptb strain that does not produce ovalbumin did not prime OT-I T cells (**Supplementary Fig. 1c**). Both Yptb-OVA and control Yptb strains were capable of priming a very strong endogenous CD8 response against the YopE<sub>69-77</sub> epitope revealed by tetramer staining<sup>14,15</sup> (**Supplementary Fig. 1c**). Importantly, the level of YopE-OVA production was sufficient to allow ovalbumin to act as a protective antigen. Mice that had been previously immunized with vesicular stomatitis virus expressing OVA (VSVOVA) were protected from Yptb-OVA challenge compared to immune mice challenged with control Yptb not expressing OVA (**Supplementary Fig. 1d**).

To more thoroughly examine the expansion and persistence of CD8 T cells, we transferred naive GFP OT-I cells, then infected mice one day later with Yptb-OVA and determined the percent of OT-I cells and YopE-tetramer positive cells among total CD8 $\alpha\beta^+$  T cells in the intestinal epithelium (IEL), lamina propria (LP), mesenteric lymph nodes (MLNs), and spleen (**Fig. 1a**) at various timepoints post infection. The expansion of OT-I T cells mirrored that of CD8 T cells specific for the endogenous YopE epitope. There were about 4-5 fold greater numbers of YopE tetramer-positive CD8 T cells than OT-I cells both during acute infection (day 9) and after bacterial clearance at day 45 (**Fig. 1a, Supplementary Fig. 2**). This huge expansion of YopE-specific cells is likely due to the high level of YopE protein production when compared to YopO<sup>20</sup>. The number of OT-I cells peaked in the MLNs at 6 days post infection, and in all other organs at day 9 (**Fig. 1b**). OT-I T cell numbers contracted and formed a stable memory population in the LP and lymphoid organs (**Fig. 1b**) that was capable of responding to rechallenge (data not shown). We saw loss of OT-I T cells in the IEL compartment over time (**Fig. 1b**, data not shown). This is unlike what is seen during systemic viral infection, where IEL numbers remain stable<sup>5</sup>; however, endogenous YopE-specific cells were also lost from the IEL suggesting this is a phenomena associated

with Yptb infection and not an artifact only observed in OT-I T cells. Overall, these data indicate transfer of OT-I T cells and Yptb-OVA infection represents a useful model for examining the intestinal CD8 T cell response to a pathogen that causes robust infection of the gut.

### A population of CD103<sup>-</sup> T<sub>RM</sub> cells develop in the LP

Yptb-specific CD8 T cell responses were most abundant in the intestinal tissue, specifically the LP, a site of *Yersinia* colonization. The phenotype and function of LP CD8 T cells has not been extensively examined, especially in the context of oral pathogens that infect this tissue. CD8 T cells that enter the intestine undergo phenotypic changes characteristic of T<sub>RM</sub> cells, including upregulation of the integrin CD103, CD69 and granzyme B<sup>5</sup>. As expected, OT-I T cells primed during Yptb-OVA infection upregulated CD103 soon after entry into the IEL compartment and the percentage of CD103<sup>+</sup> cells did not change after 9 days post infection (**Fig. 2a**). However, the LP contained a more heterogeneous population of OT-I cells; only about 50% of these cells became CD103<sup>+</sup> (**Fig. 2a**). Both CD103<sup>+</sup> and CD103<sup>-</sup> cells in the LP expressed other markers of tissue residence including CD69 and granzyme B (**Fig. 2b**, data not shown), indicating CD103<sup>-</sup> intestinal OT-I cells had undergone some of the phenotypic changes associated with T<sub>RM</sub> cells. The anti-apoptotic factor Bcl2 was also upregulated in both CD103<sup>+</sup> and CD103<sup>-</sup> LP CD8 cells (**Fig. 2c**), supporting their long-term persistence<sup>8</sup>. Although CD103 plays a role in the development and/or persistence of T<sub>RM</sub> cells in the brain<sup>21</sup>, skin<sup>8</sup>, and IEL compartment<sup>7,10</sup>, this molecule is not required for maintenance of CD8 T cells in the LP<sup>7,10</sup>.

Downregulation of the transcription factor KLF2 is observed in T<sub>RM</sub> cells and is thought to favor the establishment of this population via repression of the sphingosine 1-phosphate receptor 1 gene (*S1p1r*)<sup>12</sup>. We examined *Klf2* mRNA expression in sorted intestinal OT-I cells by qRT-PCR. CD69<sup>+</sup>CD103<sup>-</sup> LP CD8 cells failed to downregulate *Klf2* to the levels observed in CD69<sup>+</sup>CD103<sup>+</sup> LP cells (**Fig. 2d**). In fact, the expression of *Klf2* mRNA in CD103<sup>-</sup> LP CD8 cells was not significantly different from the level in splenic CD8 T cells (**Fig. 2d**). Supporting an increase in functional KLF2 protein, the expression of *S1p1r* mRNA was also increased in the CD69<sup>+</sup>CD103<sup>-</sup> LP population relative to CD69<sup>+</sup>CD103<sup>+</sup> LP and IEL OT-I cells (**Supplementary Fig. 3**). This raised the possibility that CD103<sup>-</sup> cells represent a population that is newly recruited from the circulation<sup>12</sup>. In line with this, a CD103<sup>-</sup> population of CD4 T cells that can transiently reside in the skin has been observed<sup>6</sup>. We hypothesized that if CD103<sup>-</sup> cells were transients in the LP they would be sensitive to CD8-depleting antibody treatment. To test this, 28 days after Yptb-OVA challenge, mice were treated with anti-CD8 antibodies and 7 days after treatment intestinal OT-I populations were analyzed. No difference in the ratio of CD103<sup>+</sup>:CD103<sup>-</sup> LP populations was observed (**Fig. 2e**), indicating the LP CD103<sup>-</sup> CD8 population represent true resident cells. Confirming the effectiveness of antibody depletion, there was a 500-fold reduction in the number of CD8 T cells in the spleen of treated versus untreated mice (data not shown). These data indicate infection results in a long lived subset of T<sub>RM</sub> cells that fail to express CD103 and have increased levels of *Klf2* mRNA, but upregulate other molecules associated with tissue residence including CD69, granzyme B, and Bcl2.

### CD103<sup>-</sup> LP T<sub>RM</sub> cells develop without TGF-βR signalling

TGF-βR signalling in T cells plays an important role in the upregulation of CD103<sup>7,8,11,22</sup> and repression of *Klf2*<sup>12</sup>. Failure of a subset of LP T<sub>RM</sub> cells to upregulate CD103 and downregulate *Klf2* suggests that these cells might not require TGF-β in infected intestinal tissue. To examine the role of TGF-β signals in the development of the CD103<sup>-</sup> LP CD8 T cell population, wild-type and TGF-βR-deficient (*Tgfb2* KO) OT-I T cells were transferred into mice followed by infection with Yptb-OVA. We found similar numbers of wild-type and *Tgfb2* KO OT-I T cells at acute timepoints in spleen, IEL and LP (**Fig. 3a**). After infection was resolved, wild-type cells outnumbered *Tgfb2* KO OT-I cells in both the IEL and LP, but not in the spleen (**Fig. 3a**), consistent with previously published reports<sup>7,11</sup>. We examined the persistence of wild-type and *Tgfb2* KO OT-I T cells in the CD103<sup>+</sup>CD69<sup>+</sup> and CD103<sup>-</sup>CD69<sup>+</sup> LP populations (**Fig. 3b**). As expected, *Tgfb2* KO OT-I cells were completely absent from the CD103<sup>+</sup>CD69<sup>+</sup> population (**Fig. 3b**). However, a sizable population of *Tgfb2* KO OT-I T cells developed into CD103<sup>-</sup>CD69<sup>+</sup> T<sub>RM</sub> (**Fig. 3b**), and this population remained stable when compared to the total LP OT-I population (**Fig. 3c**). We also examined the expression of *Klf2* mRNA in sorted wild-type and *Tgfb2* KO LP populations. CD103<sup>+</sup> wild-type OT-I cells had reduced *Klf2* mRNA when compared to CD103<sup>-</sup> wild-type OT-I cells. *Klf2* expression in *Tgfb2* KO OT-I cells was identical to that observed in CD103<sup>-</sup> wild-type OT-I cells (**Fig. 3d**). These data indicate that TGF-β signalling is not required for the development of CD103<sup>-</sup> LP T<sub>RM</sub>, in contrast to other intestinal populations, which require TGF-β to form long-lived T<sub>RM</sub> (**Fig. 3a**)<sup>7,11</sup>.

### Differential localization of intestinal T<sub>RM</sub> cells

Little is known about the distribution of antigen specific CD8 T cells upon colonization with an intestinal pathogen, and we hypothesized the phenotypic differences we observed may be due to different microenvironments created by Yptb infection within the intestine. We examined the localization of GFP OT-I T cells in the intestine of Yptb-OVA infected mice at 9 days post infection. The OT-I cells in the ileum of the small intestine could be divided into two groups based on their distribution: those that were present singly and evenly distributed throughout the tissue, and those that formed clusters (**Fig. 4a**). These CD8 T cell clusters were found primarily underlying the crypts; however, they could occasionally be found in the villus LP (**Fig. 4a**). We then examined the surface expression of CD103 on OT-I T cells within the intestine and found that while the majority of the uniformly distributed OT-I cells in IEL and LP expressed CD103 (**Fig. 4b** left), OT-I T cells in clusters near the crypts were mostly CD103<sup>-</sup> (**Fig. 4b** right, **Supplementary Fig. 4a**). Tissue sections were also stained with Yptb-specific antibodies, indicating OT-I T cells clustered around areas of bacterial infection (**Fig. 4c**). Similar CD8 T cell clusters were also found in the cecum and colon but not the duodenum (**Supplementary Fig. 4b-d**). This is consistent with CD8 T cell clusters indicating areas of LP infection, as Yptb infects the distal part of the small intestine, cecum, and colon, but not the proximal small intestine (**Supplementary Fig. 4e**). These data suggest recruitment to these intestinal aggregates during infection affects the phenotype and function of LP CD8 T cells, with clustered cells expressing the resident memory markers CD69 and granzyme B but not CD103.

### Clusters contain CD4 T cells and CX3CR1<sup>+</sup> cells

The intestinal distribution of CD103<sup>+</sup> and CD103<sup>-</sup> OT-I T cells during Yptb-OVA infection was distinct, and we sought to define the local immune environment in clusters that contained CD103<sup>-</sup> CD8 T cells. Isolated lymphoid follicles (ILFs) in the gut are generated soon after birth in response to microbial colonization and mature ILFs contain B cells, CD11c<sup>+</sup> dendritic cells (DCs), and a small number of lymphoid tissue inducer cells<sup>23</sup>. The M cells that overlie these structures are a major portal of Yptb entry into the intestinal tissue<sup>24,25</sup>, and pathogens such as *Salmonella* have been shown to preferentially invade ILFs<sup>26</sup>. Therefore, we hypothesized that ILFs may support Yptb invasion and/or replication and CD8 T cell clustering. To examine this, intestinal tissue sections from Yptb-OVA infected mice were stained with anti-B220 antibodies to identify B cells and colocalization with OT-I cells was assessed. We occasionally observed a small number of OT-I T cells associating with clustered B220<sup>+</sup> cells characteristic of ILFs (**Fig. 5a**), but OT-I T cell clusters contained few if any B220<sup>+</sup> cells (**Supplementary Fig. 5**). These data indicate OT-I T cell clusters are not formed in or around ILFs during Yptb-OVA infection, although OT-I cells are not excluded from these structures.

OT-I T cell clusters in the LP always contained endogenous CD8αβ T cells (**Fig. 5b**), consistent with the presence of large numbers of YopE-specific cells in the intestine. In addition, CD8 T cell clusters always contained CD4 T cells (**Fig. 5b**) and we hypothesized these CD4 T cells are also Yptb-specific as CD4 responses are generated during *Yersinia* infection and are implicated in protection<sup>27-29</sup>.

The presence of antigen-specific T cells and bacteria within these clusters suggested that they might also contain inflammatory antigen presenting cells. The intestinal LP contains a diverse population of macrophages and dendritic cells, and we sought to define these populations in naive and Yptb-OVA infected mice by flow cytometry. *Cx3cr1<sup>gfp/+</sup>* (CX3CR1-GFP) mice were used to aid in the identification of macrophage and/or DC populations<sup>30</sup>. MHC class II<sup>+</sup> cells were gated and CD11c, CD11b, CD103 and CX3CR1-GFP were used to differentiate LP macrophage and DCs into 4 populations (**Fig. 5c**). Small populations of conventional DCs (1: CD11c<sup>+</sup>CD11b<sup>-</sup>CD103<sup>+</sup>) and migratory DCs (2: CD11b<sup>+</sup>CD11c<sup>+/lo</sup>CD103<sup>+</sup>CX3CR1<sup>-</sup>) were found in naive mice, and these two populations remained stable after infection (**Fig. 5d**). In contrast, the CX3CR1-expressing subset of antigen presenting cells made up nearly 30% of MHC class II<sup>+</sup> cells in naive mice and the size of this population increased during Yptb-OVA infection. These CX3CR1 positive cells could be further subdivided into those that had been recently recruited to the intestine (3: CD11b<sup>+</sup>CD11c<sup>+/lo</sup>CD103<sup>-</sup>CX3CR1<sup>int</sup>) and resident macrophages (4: CD11b<sup>+</sup>CD11c<sup>+/lo</sup>CD103<sup>-</sup>CX3CR1<sup>hi</sup>) based on the degree of CX3CR1-GFP expression<sup>30</sup> (**Fig. 5c**). We observed that the recently recruited CX3CR1<sup>int</sup> macrophage and/or DC population increased approximately 4-fold during infection, while the resident CX3CR1<sup>hi</sup> population was unchanged (**Fig. 5d**). The CX3CR1<sup>int</sup> population has been shown to be recruited to the colon during colitis and is derived from inflammatory monocytes<sup>30</sup>. Consistent with this, during Yptb-OVA infection CX3CR1<sup>int</sup> cells retained monocytic markers including CCR2 and Ly6C (**Supplementary Fig. 6**). We hypothesized that this population of CX3CR1 positive macrophages and/or DCs would be recruited to areas of

bacterial colonization with OT-I cells, and close interactions between clustered OT-I cells and CX3CR1<sup>+</sup>CD11c<sup>+/lo</sup> cells were readily observed (**Fig. 5e, inset**). In contrast, CX3CR1<sup>-</sup>CD11c<sup>+</sup> cells were rarely associated with OT-I cells (**Fig. 5e**). These data suggest that the T cell-containing clusters represent structures formed in the intestine during local infection that contain antigen specific CD8 T cells, CD4 T cells, and resident and recruited CX3CR1<sup>+</sup> antigen presenting cells and may represent a unique microenvironment that affects the phenotype and function of LP T<sub>RM</sub> CD8 T cells. OT-I cells and endogenous CD8 cells remained clustered at 30 days post infection, when Yptb-OVA was no longer detectable in the intestinal tissue (**Supplementary Fig. 7a-c**). The clusters dispersed by 120 days post infection (**Supplementary Fig. 7b, 7d**); however, the percentage of CD103<sup>-</sup> cells in the LP remained stable (**Fig. 2a**) suggesting any effect localization has on CD8s T cells is imprinted relatively early after infection. These results suggest that clusters of antigen presenting cells, CD4 and CD8 T cells form at sites of Yptb invasion.

### CD103<sup>-</sup> T<sub>RM</sub> develop independently of local antigen

The role of antigen in the development of different tissue resident memory populations is somewhat enigmatic. Continual antigenic stimulation by self peptides has been shown to prevent CD103 expression on intestinal CD8 T cells<sup>10</sup>. In the skin, CD103 is expressed whether or not antigen is present<sup>31</sup>, while in the brain, antigen recognition is required for CD103 upregulation<sup>21</sup>. The localization of CD103<sup>-</sup> LP cells to areas containing bacterial colonization and recruited inflammatory monocytes suggest this subset of LP T<sub>RM</sub> cells may be exposed to unique signals during their development that may lead to this altered phenotype. CX3CR1<sup>int</sup> and, to a lesser extent, CX3CR1<sup>hi</sup> intestinal macrophages/dendritic cells are capable of presenting antigens and producing inflammatory cytokines in the normally immunosuppressive LP environment<sup>30,32</sup>. We hypothesized that presentation of Yptb-OVA antigens within CD8 aggregates may affect CD103 expression on clustered wild-type cells. Presentation of Yptb-OVA antigens by CX3CR1-expressing populations was assessed by sorting CX3CR1<sup>int</sup> and CX3CR1<sup>hi</sup> populations from the LP of Yptb-OVA infected mice on day 6 after infection. These cells were mixed with CFSE labelled CD44<sup>hi</sup> CD8 T cells from Yptb-OVA immune mice (that include both YopE- and OVA-specific CD8 T cells) and proliferation was examined after 3 days. We found that the CX3CR1<sup>int</sup> population from infected mice stimulated more proliferation of Yptb-OVA memory CD8s compared to the CX3CR1<sup>int</sup> population from naive mice (**Fig. 6a, 6b**). The CX3CR1<sup>hi</sup> population from infected mice stimulated some proliferation of Yptb-OVA memory CD8 cells, but the percent division was not significantly greater than that seen from the same population from uninfected mice (**Fig. 6b**). Together this indicates that CD8 T cells in clusters during *Yersinia* infection are exposed to their cognate antigen.

To more definitively examine the role of intestinal antigen presentation in regulating CD103 expression on LP CD8 T cells, mice received OT-I T cells and were infected with Yptb-OVA. Six days after infection, CD8 T cells from the spleen and MLN were transferred into congenically marked recipients that were infected with Yptb that do not express ovalbumin (Yptb-NEG). The phenotype of donor cells in the intestine was examined 9 days later. Donor cells that did not receive antigen stimulation in the second host (OT-I cells) had similar ratios of CD103<sup>+</sup>:CD103<sup>-</sup> cells as Yptb-specific donor cells (**Fig. 6c, 6d**). These data

suggested that inflammatory signals in CD8 T cell clusters, and not antigen presentation, stimulated the development of CD103<sup>-</sup> LP T<sub>RM</sub> cells.

### CXCR3 is required for CD8 T cell cluster formation

CD8 T cell clusters within the intestine may be exposed to a unique array of inflammatory cytokines produced by CX3CR1<sup>int</sup> cells at sites of local infection and this may redirect their phenotype to CD103<sup>-</sup> T<sub>RM</sub>. CXCR3 has been identified as important for localization of CD8 T cells to areas of infection in nonlymphoid tissue including the brain, lung, and female reproductive tract<sup>33-36</sup>, and we hypothesized CXCR3 may be involved in targeting CD8 T cells to areas of intestinal inflammation during Yptb-OVA infection. Expression of the CXCR3 ligands *Cxcl9* and *Cxcl10*<sup>37</sup> was examined in intestinal macrophage/DC populations. RT-PCR was performed to determine levels of chemokine expression by cell populations sorted as previously described (**Fig. 5d**). We found that *Cxcl9* mRNA expression was uniform in all populations and not upregulated during Yptb-OVA infection (**Fig. 7a**); however, *Cxcl10* mRNA was expressed at the highest level in CX3CR1-expressing populations in naive mice, and during infection expression was significantly increased in both the resident CX3CR1<sup>hi</sup> and recruited CX3CR1<sup>int</sup> population (**Fig. 7a**). Production of the CXCR3 ligand CXCL10 suggests CXCR3 may be important for localization to areas of inflammation within the intestine.

To examine the role of CXCR3 in intestinal entry and localization, an equal number of naive wild-type and CXCR3-deficient (*Cxcr3* KO) OT-I T cells were co-transferred into mice, followed by infection with Yptb-OVA. The percentage of OT-I cells from each group at 9 days post infection in the intestine and systemic tissues was examined. Wild-type and *Cxcr3* KO OT-I cells were present in similar numbers in the MLNs and spleen of infected mice (**Fig. 7b**). In the gut, we found no difference in the percentage of wild-type and *Cxcr3* KO in the IEL population, but in the LP there was a two-fold reduction in the number of *Cxcr3* KO OT-I T cells compared to wild-type (**Fig. 7b**). The distribution of OT-I cells was examined by histology, revealing that CD8 T cell clusters in the ileum contained wild-type cells but few if any *Cxcr3* KO T cells (**Fig. 7c**). In areas of the intestine without clusters of OT-I T cells, both populations were present at a similar number and distribution (**Fig. 7c**). T cell clustering was quantified by determining the number of OT-I T cells in a single villus including all underlying tissue (**Fig. 7d**), and this data was expressed as the percentage of villi containing a given number of OT-I T cells (**Fig. 7e**). 13.7% of villi contained greater than 10 wild-type OT-I cells; in contrast, we did not observe any villi containing more than 10 *Cxcr3* KO OT-I cells (**Fig. 7e**). These data indicate CXCR3 is required for migration of CD8 T cells to foci of infection but not to other areas of the intestine.

### *Cxcr3* KO T cells fail to control bacterial replication

Our data indicate that Yptb-OVA infection creates distinct microenvironments within the intestine. Wild-type OT-I cells present in CD8 T cell clusters fail to upregulate CD103 (**Fig. 4b**), and we hypothesized the exclusion of CXCR3-deficient cells from these structures may result in an altered phenotype compared to wild-type OT-I cells. To examine this, we analyzed the expression CD103 on intestinal wild-type and *Cxcr3* KO OT-I cells following Yptb-OVA infection. Yptb-OVA primed wild-type cells in the IEL compartment had



upregulated CD103, and an even higher percentage of *Cxcr3* KO IEL were CD103<sup>+</sup> (**Fig. 8a,b**). This differential phenotype was even more pronounced in the LP, with a significantly higher percentage of *Cxcr3* KO OT-I cells expressing CD103 (**Fig. 8a,b**). *Cxcr3* KO CD8 T cells displayed an increased memory precursor phenotype (KLRG1<sup>-</sup>CD127<sup>+</sup>) due to altered exposure to inflammatory cytokines during priming<sup>33,38,39</sup> (**Supplementary Fig. 8a**). It has been suggested that CD8 T cells with a memory precursor phenotype preferentially develop into CD103<sup>+</sup> T<sub>RM</sub> cells<sup>7,8</sup>. However, *in vitro* activation of wild-type and *Cxcr3* KO OT-I T cells allows similar access to inflammatory cytokines<sup>38</sup> and when *in vitro* activated OT-I cells were transferred into Yptb-OVA infected mice we still observed increased CD103-expression on intestinal *Cxcr3* KO OT-I cells compared to wild-type OT-I cells (**Supplementary Fig. 8b**). It was conceivable that exposure of recruited CD8 T cells to CXCL10 in the tissue may directly modulate their expression of CD103. To examine this, wild-type and *Cxcr3* KO effector OT-I cells were stimulated with TGF- $\beta$  *ex vivo*, which resulted in upregulation of CD103 expression in both wild-type and *Cxcr3* KO OT-I cells (**Supplementary Fig. 8c**).

Addition of CXCL10 to the culture did not prevent CD103 upregulation in response to TGF- $\beta$  (**Supplementary Fig. 8c**), indicating CXCR3 signaling did not directly regulate CD103 expression. Together these data suggest that during intestinal infection localization to these lymphoid clusters alters the expression of a subset of T<sub>RM</sub> cell markers including CD103 and CXCR3-mediated trafficking plays a critical role in establishing this population.

*Cxcr3* KO OT-I cells in the LP fail to localize to lymphoid clusters and develop almost exclusively into the CD103<sup>+</sup>CD69<sup>+</sup> subset, and we used this to analyze the contribution of this population to controlling bacterial replication in the LP. CD90.1 mice were T cell depleted and infected with Yptb-OVA. Two days later mice received CD4 T cells from Yptb-infected CD90.2 wild-type mice and CD8 T cells from either CD90.2 wild-type or *Cxcr3* KO mice. Three days after T cell transfer colony-forming units (CFU) in the intestine and spleen were quantified. We found a significant decrease in the bacterial burden in the ileum of mice receiving wild-type T cells, but not those receiving *Cxcr3* KO T cells (**Fig. 8c**). Wild-type and *Cxcr3* KO CD8 T cell transfers did reduce CFU in the spleens (**Fig. 8c**), although this did not reach statistical significance. Together these data suggest that CXCR3 regulates differentiation of CD103<sup>-</sup>CD69<sup>+</sup> LP CD8 cells by altering their localization within the intestine, and that this T<sub>RM</sub> cell subset is superior at limiting bacterial replication in the gut.

## Discussion

CD103<sup>-</sup> T<sub>RM</sub> cells have been observed in a variety tissues; however, the abundance of this population varies by location, nature of infection, and availability of antigen<sup>10,21</sup>. It is often speculated that these cells are in a transitional phase and will eventually become CD103<sup>+</sup> or are circulating cells that are only transiently present in the tissue<sup>6</sup>. Here we identify a stable population of LP CD103<sup>-</sup> T<sub>RM</sub> cells that develop after Yptb infection; these cells are distinct from CD103<sup>+</sup> intestinal CD8 cells in both their phenotype and requirements for inflammatory signals within the intestine. CD103<sup>-</sup> T<sub>RM</sub> cells do not require TGF- $\beta$ R signalling, unlike CD103<sup>+</sup> cells in both the IEL and LP compartments. CD103<sup>-</sup> LP CD8

cells cluster in areas of infection with other resident and recruited immune cells including inflammatory monocyte-derived antigen presenting cells and antigen specific T cells. CD103<sup>-</sup> CD8 cells localize in areas that are abundant in antigen, which can affect CD103 expression on CD8 T cells<sup>10</sup>. However, in the LP, antigen did not alter the development of CD103<sup>-</sup> T<sub>RM</sub> cells, implicating inflammatory signals in this process. *Cxcr3* KO CD8 T cells were not recruited to areas of infection, and accordingly, were skewed to the CD103<sup>+</sup> phenotype and they were unable to control bacterial replication. These data identify intestinal CD103<sup>-</sup> LP CD8 cells as developmentally distinct from their CD103<sup>+</sup> counterparts, and indicate T<sub>RM</sub> cells are heterogeneous and have distinct functions during infection.

The formation of intestinal CD8 T<sub>RM</sub> cells is negatively affected by the loss of TGF- $\beta$  signalling<sup>7,10,11</sup>; however, cells in the LP are not as sensitive to loss of TGF- $\beta$ -dependent signals as those in the IEL<sup>7,11</sup>. The LP population that persists in the absence of TGF- $\beta$  signalling is analogous to the CD103<sup>-</sup> CD8 population that develops in a wild-type setting. It is possible these cells fail to receive TGF- $\beta$  signals; however, Yptb effectors all respond to TGF- $\beta$  stimulation *ex vivo*, expression of *Tgfb* is increased in CX3CR1<sup>+</sup> cells during infection, and both CD103<sup>+/-</sup> LP populations express equivalent amounts of *Tgfb*2 (data not shown). TGF- $\beta$  is maintained in a latent form and requires activation by integrins or proteases<sup>40</sup> and local production of these activating factors could be altered during infection thus regulating the availability of active TGF- $\beta$ .

An alternative possibility is that CD8 T cells that enter the intestine are responsive to and exposed to active TGF- $\beta$ , but other signals change the differentiation pattern of these cells. Intestinal antigen has been suggested to alter CD103 expression *in vivo*<sup>10</sup>; however, antigen does not downmodulate CD103 expression in the context of Yptb infection. There is evidence that exposure of CD8 effectors to TGF- $\beta$  in the presence of inflammatory cytokines like IL-33 or type I IFN prevents CD103 upregulation<sup>10</sup>. Although this does not explain the differential expression of *Klf2*, as both these cytokines synergize with TGF- $\beta$  to stimulate *Klf2* downregulation<sup>12</sup>. Further experiments are needed to determine if TGF- $\beta$  receptor signaling has been activated in CD103<sup>-</sup> populations and what specific inflammatory signals drive their development. The CX3CR1<sup>int</sup> DC population that is a major component of intestinal aggregates has a unique cytokine profile that is more inflammatory than resident intestinal macrophage populations and during colitis this subset is capable of producing IL-6 and IL-23<sup>30</sup>. In addition, both the CX3CR1<sup>int</sup> and CX3CR1<sup>hi</sup> population have increased expression of IL-1<sup>30</sup>, and these cytokines have all been implicated in the host response to *Yersinia* infection<sup>41-44</sup>. Determining the inflammatory cytokine profile of CX3CR1<sup>+</sup> populations within CD8 T cell clusters would aid in identifying which cytokines intestinal T cell populations are exposed to during infection.

CD8 T<sub>RM</sub> cells in the female reproductive tract and skin act as an alarm upon antigen re-exposure, rapidly recruiting circulating memory CD8 T cells and other immune cells and inducing an antimicrobial state within the tissue<sup>36,45,46</sup>. The evenly distributed CD103<sup>+</sup> CD8 cells we observe in the intestine are ideally positioned to carry out this alarm function, as they are present throughout the tissue and develop independently of the nature of the pathogenic insult. On the other hand, CD103<sup>-</sup> CD8s develop around sites of infection within

the tissue and have an immediate effect during primary infection, but their role in combating reinfection is unclear. We hypothesize that instead of affecting tissue residence, CD103 regulates migration within the intestinal tissue and its absence allows these cells to home to areas of infection, as they are not tethered to E-cadherin expressing cells. There is little data addressing the migration of T cells within the intestine at steady state or during infection; however, rapid migration of memory T cells has been observed within the dermis<sup>47</sup> suggesting T<sub>RM</sub> cells are not always restricted in their movement. CD8 T cell clusters eventually dissipate without affecting the size of the CD103<sup>-</sup> pool, suggesting these cells are capable of moving within the LP. We speculate that CD103<sup>+</sup> IEL and LP populations are poised to raise the alarm to reinfection and CD103<sup>-</sup> LP CD8 cells are able to migrate to foci of infection. Circulating memory cells do not express molecules ( $\alpha_4\beta_7$  and CCR9) that allow them to enter intestinal tissue<sup>4</sup>; therefore, cells that rapidly control local infection would have to be present within intestinal tissue. The ability of CD8 T cells to wall off areas of bacterial infection and control their replication may be critical, as *Yptb* and other bacterial pathogens can seed systemic organs directly from the intestine<sup>16,17</sup> and formation of these structures could prevent reintroduction into the lumen of the intestine as well as access to the blood or lymph vessels that are abundant in the LP.

Overall these data suggest *Yptb* infection provides a useful model for examining the recruitment of CD8 T cells to the intestine and how distinct microenvironments within this tissue can instruct their development into unique intestinal CD8 T<sub>RM</sub> cell subsets. Studies comparing the profiles of CD8 cells from different tissues suggested only a small number of genes represent the core transcriptional changes that dictate T<sub>RM</sub> cell formation<sup>8</sup>. Differentiating between CD103<sup>+</sup> and CD103<sup>-</sup> CD8 populations may be important in analyzing transcriptional signatures as these two populations are exposed to different signals within the tissue<sup>9</sup>.

## METHODS

### Bacteria

*Yersinia pseudotuberculosis* YPIII was modified using allelic exchange to generate *Yptb*-OVA. A *YopE*::OVA fusion construct was generated by amplifying a fragment of ovalbumin from nucleotides 742-1068 followed by a stop codon (5'-TCTAGAGATGAAGTCTCAGGCCTTGAG-3', 5'-GGATCCCTAAGACGCTTGCAGCATCCACTC-3') and inserting it into the *Xba*I and *Bam*HI sites of *pYopE*::*Cya*<sup>48</sup> which contained the first 390 nucleotides of *YopE*. This *YopE*::OVA fusion construct was amplified (5'-AGATCTATGAAAATATCATCAT-3', 5'-AGATCTAAGACGCTTGCAGCA-3') and cloned into the *Bgl*III site of the *pYopO* $\delta$ 1-2199 suicide vector plasmid<sup>49</sup>. Allelic exchange was performed as described<sup>50</sup>. Replacement of the *YopO* gene with *YopE*::OVA was confirmed by PCR and sequencing.

### Mice and infections

C57BL/6, *Cxcr3*<sup>-/-</sup> and *Cx3cr1*<sup>gfp/gfp</sup> mice were obtained from Jackson Laboratories and housed in specific pathogen-free conditions at the University of Washington animal facilities. OT-I T cell receptor transgenic mice were maintained in the same facility and

crossed to *Cxcr3*<sup>-/-</sup> mice. *Tbfb $\beta$ R2*<sup>fl/fl</sup> dLck-cre OT-I mice<sup>51</sup> were previously described. All experiments were done in accordance with the Institutional Animal Care and Use Committee guidelines of the University of Washington. Naive OT-I T cells were isolated from the spleen and lymph nodes using a CD8 T cell isolation kit (Miltenyi) with the addition of biotinylated anti-CD44 antibody. Mice received congenically marked naive OT-I T cells intravenously and one day later were infected with  $2 \times 10^8$  Yptb-OVA in 150 $\mu$ l PBS by oral gavage when indicated. CD8 T cells were depleted by intraperitoneal injection of 150 $\mu$ g anti-CD8 $\alpha$  antibody (2.4.3) one week prior to analysis.

For effector CD8 transfer experiments, CD45.2 mice were given CD45.1/2 OT-I T cells and infected with Yptb-OVA. Six days after infection, cells from the mesenteric lymph nodes and spleen were isolated and CD8s were enriched by depletion of CD4 and CD19 expressing cells. Enriched CD8s were injected into CD45.1 mice that had been infected with Yptb-NEG 6 days prior; each recipient mouse was injected with the total cells isolated from a single donor mouse. LP and IEL cells were examined 9 days after transfer.

For protection experiments, CD90.1 recipient mice were given 200 $\mu$ g anti-CD90.1 (19E12) intraperitoneally at the time of infection followed by an additional 200 $\mu$ g every other day. Wild-type and *Cxcr3* KO T cells (day 7 Yptb-OVA effectors) were sorted from CD90.2 donor mice and transferred into recipient mice on day 2. Each recipient mouse received  $7.5 \times 10^5$  total wild-type CD4 T cells and  $7.5 \times 10^5$  wild-type or *Cxcr3* KO CD8 T cells. Wild-type and *Cxcr3* KO donor populations had equivalent numbers of YopE-specific cells and expressed similar amounts of  $\alpha_4\beta_7$ . Three days after T cell transfer, tissues were isolated and homogenized in PBS. Tissue homogenates were plated on cefsulodin-novobiocin-irgasan (CIN) agar (BD Biosciences) and data are expressed as the total number of colony forming units (CFU) per organ.

For *in vitro* activation experiments, OT-I cells were activated with splenocytes pulsed with 1 $\mu$ M SIINFEKL in the presence of 100ng/ml LPS. Twenty U/ml IL-2 was added daily beginning on day 2. Four days after activation, cells were purified using Histopaque 1083 (Sigma) and  $1-2 \times 10^6$  cells were injected i.v. into day 5 Yptb-OVA infected mice. Cells were analyzed 4 days after transfer.

**Isolation of intestinal cells**—To isolate intestine IEL and LP cells, Peyer's patches were removed, the intestine was cut open longitudinally, and intestinal contents and mucus were removed by gentle scraping. The intestine was cut into 1cm pieces and incubated in HBSS buffer containing 1mM dithiothreitol and 10% FBS at 37°C with stirring for 20 minutes to isolate IELs. Intestinal tissue was transferred to HBSS containing 1.3mM EDTA and stirred at 37°C for 20 minutes to remove the epithelium. Intestinal pieces were then incubated in HBSS containing 5% FBS and 150U/ml collagenase type 2 (Worthington) at 37°C with stirring for 45 minutes to isolate LP cells. IEL and LP cells were further purified by gradient centrifugation with 44% and 67% Percoll.

## Flow cytometry

Single cell suspensions from lymph nodes, spleen, and intestine were isolated at indicated timepoints post infection and stained with antibodies for CD8 $\beta$  (H35-17.2), CD103 (2E7),

CD69 (H1.2F3), Bcl2 (100), CD45.1 (A20), CD45.2 (104), CD90.1 (HIS51), Ly6C (AL-21), I-A<sup>b</sup> (AF6-120.1), CD11c (N418), CD11b (M1/70), CD127 (A7R34), KLRG1 (2F1), CCR9 (CW-1.2),  $\alpha_4\beta_7$  (DATK32), and F4/80 (BM8) (eBioscience, BioLegend, and BD Biosciences) and YopE<sub>69-77</sub> MHC class I tetramer (Fred Hutchinson Cancer Research Center Tetramer Core Facility). Cells were analyzed with a FACSCanto (BD) and analyzed with FlowJo software (TreeStar).

### Immunohistochemistry and microscopy

Intestinal tissues were fixed in 4% paraformaldehyde, rehydrated in 20% sucrose, and frozen in OCT media (Sakura). Tissues were cut into 7-8 $\mu$ m sections and treated with ice cold acetone. Sections were treated with biotin-avidin blocking reagent when necessary (Vector labs) and stained with the following biotinylated or directly conjugated antibodies: CD8 $\beta$  (YTS156.7.7, Biolegend), CD4 (RM4-5, eBioscience), CD103 (M290, BD Biosciences), CD90.1 (HIS5.1, eBioscience), Epcam (G8.8, Biolegend), CD11c (HL3, BD Biosciences), B220 (RA3-6B2, eBioscience). Rabbit anti-*Yersinia pseudotuberculosis* (ab26120, Abcam) and anti-rabbit Dylight 649 (ab96926, Abcam) were used to stain for bacterial antigens. Stained slides were mounted with Prolong Gold antifade reagent (Invitrogen), imaged using a Nikon 90i, and analyzed using Adobe Photoshop software.

The number of OT-I cells/villus was determined by sectioning a 'Swiss roll'<sup>52</sup> of the distal third of the small intestine. Five or more sections/mouse that were at least 400 $\mu$ m apart were stained and imaged. A villus and the underlying submucosa and muscularis were considered a single villus, and the number of OT-I cells in each region was determined. The number of OT-I cells/villus were binned and plotted as the percentage of villi containing a given range of OT-I cells.

### Quantitative RT-PCR

*Cx3cr1<sup>gfp/+</sup>* mice were infected with  $2 \times 10^8$  Yptb-OVA, and on day 7 post infection the LP cells were isolated from the ileum. Cells were stained with antibodies for CD11c, CD11b, CD103, and I-A<sup>b</sup>. CD8 T cells were isolated from tissues at various timepoints post infection and stained with antibodies for CD8 $\beta$ , CD69, CD103, and CD45.1/2. Cells were sorted using a FACSARIA (BD) to greater than 96% purity. IEL CD8 populations were defined as CD69<sup>+</sup>CD103<sup>+</sup>, and LP CD8s were sorted into CD69<sup>+</sup>CD103<sup>-</sup> and CD69<sup>+</sup>CD103<sup>+</sup> populations. RNA was isolated using an RNeasy RNA isolation kit (QIAGEN) and amplified using SYBR one step RT-PCR kit (QIAGEN) with previously described primers for *Cxcl9/Cxcl10*<sup>53</sup> and *Klf2/Slp1r*<sup>12</sup>; *actb* expression was used as a normalization control (*actb*F: 5'-GGCTGTATTCCCCTCCATCG-3', *actb*R: 5'-CCAGTTGGTAACAATGCCATGT-3').

### Ex vivo stimulation assays

Mice received wild-type and *Cxcr3* KO OT-I cells and infected as described above, and mesenteric lymph nodes were isolated on day 5 postinfection. Single cell suspensions of bulk LN cells were cultured at  $1 \times 10^6$  cells/well of a 96 well plate in RPMI 1640 supplemented with 10% FBS, 5mM L-glutamine, 55 $\mu$ M  $\beta$ -mercaptoethanol, 1mM sodium pyruvate, 10mM HEPES, 1x MEM non-essential amino acids (Invitrogen), 100 $\mu$ g/ml

streptomycin, and 100U/ml penicillin with or without 2.5ng/ml TGF- $\beta$ 1 (R&D Systems) and 25ng/ml CXCL10 (Peprotech) for 20 hours. Cells were stained for surface markers in the presence of a fixable live/dead stain (Invitrogen) to exclude dead cells.

### Ex vivo presentation assays

*Cx3cr1<sup>gfp/+</sup>* mice were infected with  $2 \times 10^8$  Yptb-OVA, and on day 6 post infection LP cells were isolated from the ileum and cecum. Cells were stained with antibodies for CD11c, CD11b, I-A<sup>b</sup> and dump gate (CD103, IgA (AD3, LSBio), CD19 (1D3, eBioscience), TCR $\beta$  (H57-597, eBioscience), TCR $\gamma\delta$  (GL3, eBioscience)) sorted using a FACS Aria (BD) to greater than 96% purity. Congenically marked CD8<sup>+</sup>CD44<sup>hi</sup> memory cells were sorted from Yptb-OVA memory mice and labelled with CFSE.  $5 \times 10^4$  APCs and  $5 \times 10^4$  memory T cells were mixed and incubated for 3 days with the addition of 5U/ml IL-2 for the final day of incubation. CFSE dilution was examined by flow cytometry and a live/dead stain was used to exclude dead cells from the analysis. Yptb- OVA memory cells were also incubated with APCs pulsed with SIINFEKL and YopE<sub>69-77</sub> peptides to determine the maximum antigen specific response, and 60-70% of sorted Yptb-OVA memory cells divided in response to this peptide mixture.

### Statistical analysis

Differences between experimental groups were analyzed using the student's *t*-test, and chi-squared test was used to analyze OT-I distribution within the tissue.

### Supplementary Material

Refer to Web version on PubMed Central for supplementary material.

### Acknowledgements

TB is supported by the Irvington Postdoctoral Fellowship from the Cancer Research Institute. This work was supported by the Howard Hughes Medical Institute and National Institutes of Health Grants AI-19335 (to MJB). We thank Mary Chase and Xiao Cun-Pan for technical assistance and Nu Zhang for critical reading of the manuscript.

### References

1. Masopust D, Vezys V, Marzo AL, Lefrancois L. Preferential localization of effector memory cells in nonlymphoid tissue. *Science*. 2001; 291:2413–2417. [PubMed: 11264538]
2. Johansson-Lindbom B, et al. Selective generation of gut tropic T cells in gut-associated lymphoid tissue (GALT): requirement for GALT dendritic cells and adjuvant. *J. Exp. Med.* 2003; 198:963–969. [PubMed: 12963696]
3. Mora JR, et al. Selective imprinting of gut-homing T cells by Peyer's patch dendritic cells. *Nature*. 2003; 424:88–93. [PubMed: 12840763]
4. Masopust D, et al. Dynamic T cell migration program provides resident memory within intestinal epithelium. *J. Exp. Med.* 2010; 207:553–564. [PubMed: 20156972]
5. Masopust D, Vezys V, Wherry EJ, Barber DL, Ahmed R. Cutting edge: Gut microenvironment promotes differentiation of a unique memory CD8 T cell population. *J. Immunol.* 2006; 176:2079–2083. [PubMed: 16455963]
6. Mueller SN, Gebhardt T, Carbone FR, Heath WR. Memory T cell subsets, migration patterns, and tissue residence. *Annu. Rev. Immunol.* 2013; 31:137–161. [PubMed: 23215646]

7. Sheridan BS, et al. Oral infection drives a distinct population of intestinal resident memory CD8(+) T cells with enhanced protective function. *Immunity*. 2014; 40:747–757. [PubMed: 24792910]
8. Mackay LK, et al. The developmental pathway for CD103(+)CD8(+) tissue-resident memory T cells of skin. *Nat. Immunol.* 2013; 14:1294–+. [PubMed: 24162776]
9. Wakim LM, et al. The molecular signature of tissue resident memory CD8 T cells isolated from the brain. *J. Immunol.* 2012; 189:3462–3471. [PubMed: 22922816]
10. Casey KA, et al. Antigen-Independent Differentiation and Maintenance of Effector-like Resident Memory T Cells in Tissues. *J. Immunol.* 2012; 188:4866–4875. [PubMed: 22504644]
11. Zhang N, Bevan MJ. Transforming growth factor- $\beta$  signaling controls the formation and maintenance of gut-resident memory T cells by regulating migration and retention. *Immunity*. 2013; 39:687–696. [PubMed: 24076049]
12. Skon CN, et al. Transcriptional downregulation of *S1pr1* is required for the establishment of resident memory CD8+ T cells. *Nat. Immunol.* 2013; 14:1285–1293. [PubMed: 24162775]
13. Bergman MA, Loomis WP, Meccas J, Starnbach MN, Isberg RR. CD8(+) T Cells Restrict *Yersinia pseudotuberculosis* Infection: Bypass of Anti-Phagocytosis by Targeting Antigen-Presenting Cells. *PLoS Pathog.* 2009; 5
14. Lin J-S, Szaba FM, Kummer LW, Chromy BA, Smiley ST. *Yersinia pestis* YopE Contains a Dominant CD8 T Cell Epitope that Confers Protection in a Mouse Model of Pneumonic Plague. *J. Immunol.* 2011; 187:897–904. [PubMed: 21653834]
15. Zhang Y, et al. A Protective Epitope in Type III Effector YopE Is a Major CD8 T Cell Antigen during Primary Infection with *Yersinia pseudotuberculosis*. *Infect. Immun.* 2012; 80:206–214. [PubMed: 22064714]
16. Barnes PD, Bergman MA, Meccas J, Isberg RR. *Yersinia pseudotuberculosis* disseminates directly from a replicating bacterial pool in the intestine. *J. Exp. Med.* 2006; 203:1591–1601. [PubMed: 16754724]
17. Melton-Witt JA, Rafelski SM, Portnoy DA, Bakardjiev AI. Oral Infection with Signature-Tagged *Listeria monocytogenes* Reveals Organ-Specific Growth and Dissemination Routes in Guinea Pigs. *Infect. Immun.* 2012; 80:720–732. [PubMed: 22083714]
18. Wiedig CA, Kramer U, Garbom S, Wolf-Watz H, Autenrieth IB. Induction of CD8(+) T cell responses by *Yersinia* vaccine carrier strains. *Vaccine.* 2005; 23:4984–4998. [PubMed: 15985316]
19. Logsdon LK, Meccas J. Requirement of the *Yersinia pseudotuberculosis* effectors YopH and YopE in colonization and persistence in intestinal and lymph tissues. *Infect. Immun.* 2003; 71:4595–4607. [PubMed: 12874339]
20. Cornelis GR, et al. The virulence plasmid of *Yersinia*, an antihost genome. *Microbiol. Mol. Biol. Rev.* 1998; 62:1315–1352. [PubMed: 9841674]
21. Wakim LM, Woodward-Davis A, Bevan MJ. Memory T cells persisting within the brain after local infection show functional adaptations to their tissue of residence. *Proc. Natl. Acad. Sci. U.S.A.* 2010; 107:17872–17879. [PubMed: 20923878]
22. El-Asady R, et al. TGF- $\beta$ -dependent CD103 expression by CD8(+) T cells promotes selective destruction of the host intestinal epithelium during graft-versus-host disease. *J. Exp. Med.* 2005; 201:1647–1657. [PubMed: 15897278]
23. Bouskra D, et al. Lymphoid tissue genesis induced by commensals through NOD1 regulates intestinal homeostasis. *Nature.* 2008; 456:507–510. [PubMed: 18987631]
24. Clark MA, Hirst BH, Jepson MA. M-cell surface beta 1 integrin expression and invasin-mediated targeting of *Yersinia pseudotuberculosis* to mouse Peyer's patch M cells. *Infect. Immun.* 1998; 66:1237–1243. [PubMed: 9488419]
25. Jang MH, et al. Intestinal villous M cells: An antigen entry site in the mucosal epithelium. *Proc. Natl. Acad. Sci. U.S.A.* 2004; 101:6110–6115. [PubMed: 15071180]
26. Halle S, et al. Solitary intestinal lymphoid tissue provides a productive port of entry for *Salmonella enterica* serovar Typhimurium. *Infect. Immun.* 2007; 75:1577–1585. [PubMed: 17283101]
27. Autenrieth IB, Tingle A, Reske-Kunz A, Heesemann J. T lymphocytes mediate protection against *Yersinia enterocolitica* in mice: characterization of murine T-cell clones specific for *Y. enterocolitica*. *Infect. Immun.* 1992; 60:1140–1149. [PubMed: 1541529]

28. Philipovskiy AV, Smiley ST. Vaccination with live *Yersinia pestis* primes CD4 and CD8 T cells that synergistically protect against lethal pulmonary *Y. pestis* infection. *Infect. Immun.* 2007; 75:878–885. [PubMed: 17118978]
29. Parent MA, et al. Cell-mediated protection against pulmonary *Yersinia pestis* infection. *Infect. Immun.* 2005; 73:7304–7310. [PubMed: 16239527]
30. Zigmond E, et al. Ly6C hi monocytes in the inflamed colon give rise to proinflammatory effector cells and migratory antigen-presenting cells. *Immunity.* 2012; 37:1076–1090. [PubMed: 23219392]
31. Mackay LK, et al. Long-lived epithelial immunity by tissue-resident memory T (TRM) cells in the absence of persisting local antigen presentation. *Proc. Natl. Acad. Sci. U.S.A.* 2012; 109:7037–7042. [PubMed: 22509047]
32. Schulz O, et al. Intestinal CD103+, but not CX3CR1+, antigen sampling cells migrate in lymph and serve classical dendritic cell functions. *J. Exp. Med.* 2009; 206:3101–3114. [PubMed: 20008524]
33. Kohlmeier JE, et al. Inflammatory chemokine receptors regulate CD8(+) T cell contraction and memory generation following infection. *J. Exp. Med.* 2011; 208:1621–1634. [PubMed: 21788409]
34. Harris TH, et al. Generalized Lévy walks and the role of chemokines in migration of effector CD8+ T cells. *Nature.* 2012; 486:545–548. [PubMed: 22722867]
35. Nakanishi Y, Lu B, Gerard C, Iwasaki A. CD8(+) T lymphocyte mobilization to virus-infected tissue requires CD4(+) T-cell help. *Nature.* 2009; 462:510–513. [PubMed: 19898495]
36. Schenkel JM, Fraser KA, Vezys V, Masopust D. Sensing and alarm function of resident memory CD8(+) T cells (vol 14, pg 509, 2013). *Nat. Immunol.* 2013; 14:876–876.
37. Groom JR, Luster AD. CXCR3 ligands: redundant, collaborative and antagonistic functions. *Immunol. Cell Biol.* 2011; 89:207–215. [PubMed: 21221121]
38. Kurachi M, et al. Chemokine receptor CXCR3 facilitates CD8(+) T cell differentiation into short-lived effector cells leading to memory degeneration. *J. Exp. Med.* 2011; 208:1605–1620. [PubMed: 21788406]
39. Hu JK, Kagari T, Clingan JM. Expression of chemokine receptor CXCR3 on T cells affects the balance between effector and memory CD8 T-cell generation. *Proc. Natl. Acad. Sci. U.S.A.* 2011; 108:E118–27. [PubMed: 21518913]
40. Travis MA, Sheppard D. TGF- $\beta$  activation and function in immunity. *Annu. Rev. Immunol.* 2014; 32:51–82. [PubMed: 24313777]
41. Dube PH, Revell PA, Chaplin DD, Lorenz RG, Miller VL. A role for IL-1 alpha in inducing pathologic inflammation during bacterial infection. *Proc. Natl. Acad. Sci. U.S.A.* 2001; 98:10880–10885. [PubMed: 11526216]
42. DePaolo RW, et al. A specific role for TLR1 in protective T(H)17 immunity during mucosal infection. *J. Exp. Med.* 2012; 209:1437–1444. [PubMed: 22778390]
43. Dube PH, Handley SA, Lewis J, Miller VL. Protective role of interleukin-6 during *Yersinia enterocolitica* infection is mediated through the modulation of inflammatory cytokines. *Infect. Immun.* 2004; 72:3561–3570. [PubMed: 15155665]
44. Jung C, et al. *Yersinia pseudotuberculosis* disrupts intestinal barrier integrity through hematopoietic TLR-2 signaling. *J. Clin. Invest.* 2012; 122:2239–2251. [PubMed: 22565313]
45. Schenkel JM, et al. T cell memory. Resident memory CD8 T cells trigger protective innate and adaptive immune responses. *Science.* 2014; 346:98–101. [PubMed: 25170049]
46. Ariotti S, et al. T cell memory. Skin-resident memory CD8<sup>+</sup> T cells trigger a state of tissue-wide pathogen alert. *Science.* 2014; 346:101–105. [PubMed: 25278612]
47. Gebhardt T, et al. Different patterns of peripheral migration by memory CD4(+) and CD8(+) T cells. *Nature.* 2011; 477:216–U119. [PubMed: 21841802]
48. Bergsbaken T, Cookson BT. Macrophage activation redirects *Yersinia*-infected host cell death from apoptosis to caspase-1-dependent pyroptosis. *PLoS Pathog.* 2007; 3:1570–1582.
49. Viboud GI, So S, Ryndak MB, Bliska JB. Proinflammatory signalling stimulated by the type III translocation factor YopB is counteracted by multiple effectors in epithelial cells infected with *Yersinia pseudotuberculosis*. *Molecular Microbiology.* 2003; 47:1305–1315. [PubMed: 12603736]



50. Palmer LE, Hobbie S, Galan JE, Bliska JB. YopJ of *Yersinia pseudotuberculosis* is required for the inhibition of macrophage TNF- $\alpha$  production and downregulation of the MAP kinases p38 and JNK. *Molecular Microbiology*. 1998; 27:953–965. [PubMed: 9535085]
51. Zhang N, Bevan MJ. TGF- $\beta$  signaling to T cells inhibits autoimmunity during lymphopenia-driven proliferation. *Nat. Immunol.* 2012; 13:667–673. [PubMed: 22634866]
52. Moolenbeek C, Ruitenber EJ. The ‘Swiss roll’: a simple technique for histological studies of the rodent intestine. *Lab. Anim.* 1981; 15:57–59. [PubMed: 7022018]
53. Sung JH, et al. Chemokine guidance of central memory T cells is critical for antiviral recall responses in lymph nodes. *Cell.* 2012; 150:1249–1263. [PubMed: 22980984]

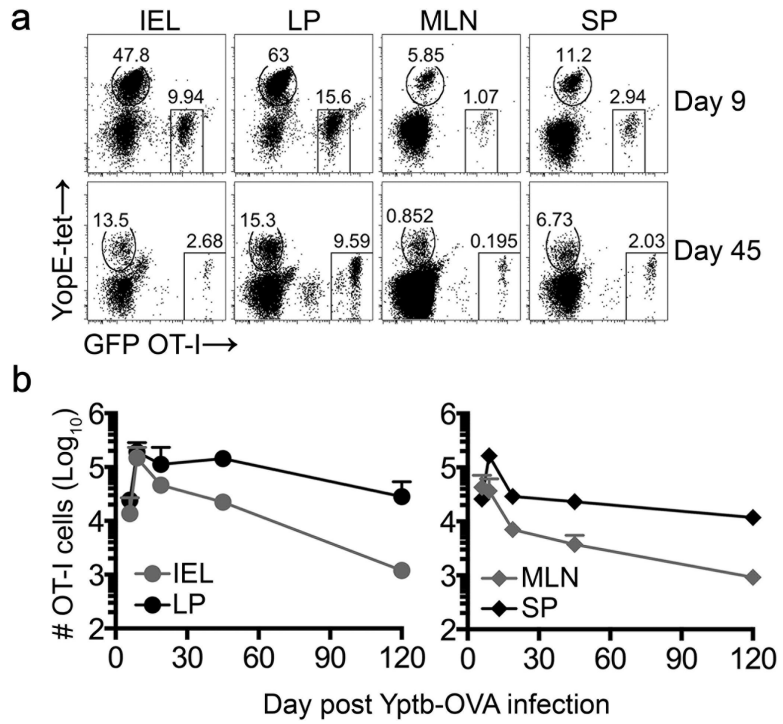


**Figure 1.** Oral Yptb-OVA infection generates a robust intestinal CD8 T cell response. C57BL/6 mice received  $1 \times 10^4$  GFP OT-I T cells and one day later were infected with  $2 \times 10^8$  Yptb-OVA. **(a)** Frequency of OT-I cells and YopE<sub>69-77</sub>-tetramer<sup>+</sup> CD8 T cells in the intestinal epithelium (IEL), lamina propria (LP), mesenteric lymph node (MLN) and spleen (SP) at 9 and 45 days after infection. Representative of 3 independent experiments. **(b)** Quantification of the total number of cells in the same tissues as in **(a)** at various timepoints post-infection. Data are means and SDs pooled from 2 experiments, with at least 3 mice/timepoint.

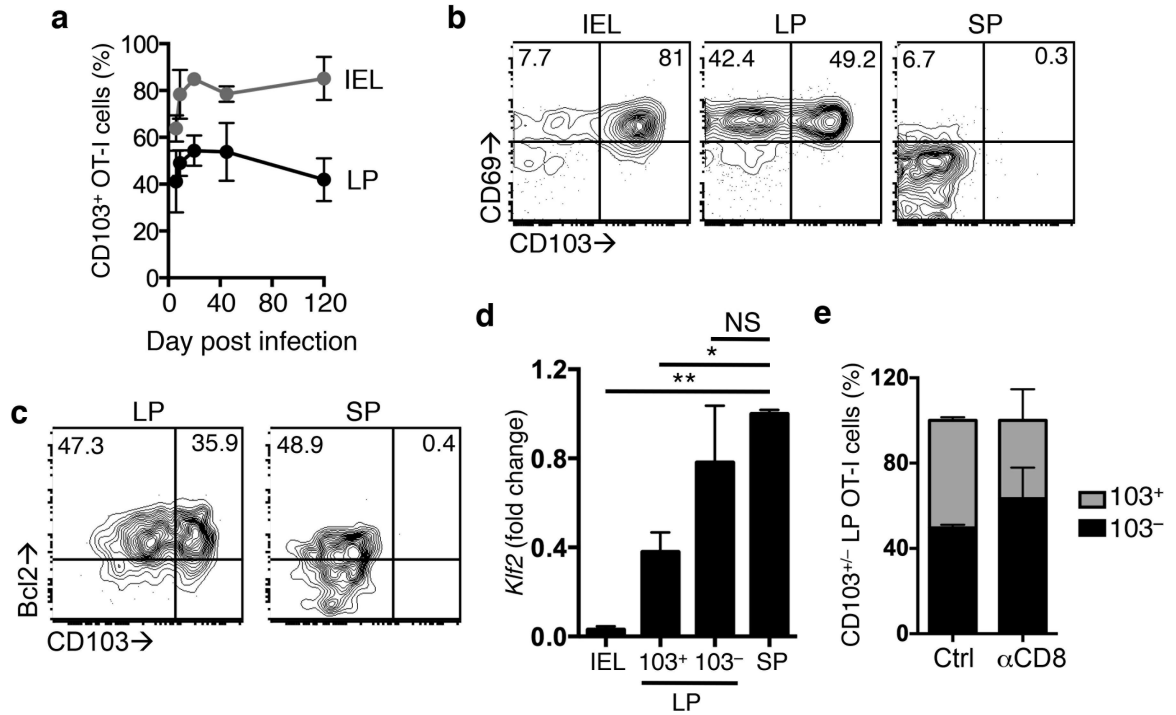


**Figure 2.** CD103<sup>-</sup> CD8 populations develop in the LP and have features of resident memory cells.  $1 \times 10^4$  congenically marked OT-I cells were transferred into C57BL/6 mice and one day later mice were infected with Yptb-OVA. **(a)** CD103 expression on OT-I T cells in the IEL and LP compartments at the indicated timepoints post infection. Data are means and SDs pooled from 3 or more mice from at least 2 independent experiments. Expression of CD103 and CD69 **(b)** or Bcl-2 **(c)** by OT-I T cells. Representative plots from 14 days **(b)** and 28 days **(c)** post infection. Representative of at least 2 experiments with 3 or more mice per group **(a-c)**. **(d)** The indicated CD8 populations were sorted from Yptb-OVA infected mice at greater than 28 days post infection. RNA was isolated and *Klf2* expression was determined using qRT-PCR and levels were normalized to *Actb* expression. Data are pooled from 2 independent biological replicates. \* $p < 0.01$ , \*\* $p < 0.001$  when compared to splenic CD8 cells (paired *t*-test). **(e)** At 28 days post infection, mice were treated intraperitoneally with 150  $\mu$ g of anti-CD8 $\alpha$  depleting antibody. Seven days after treatment, CD103 expression was determined for LP OT-I T cells. Data are means and SDs pooled from 3 or more mice from at least 2 independent experiments.

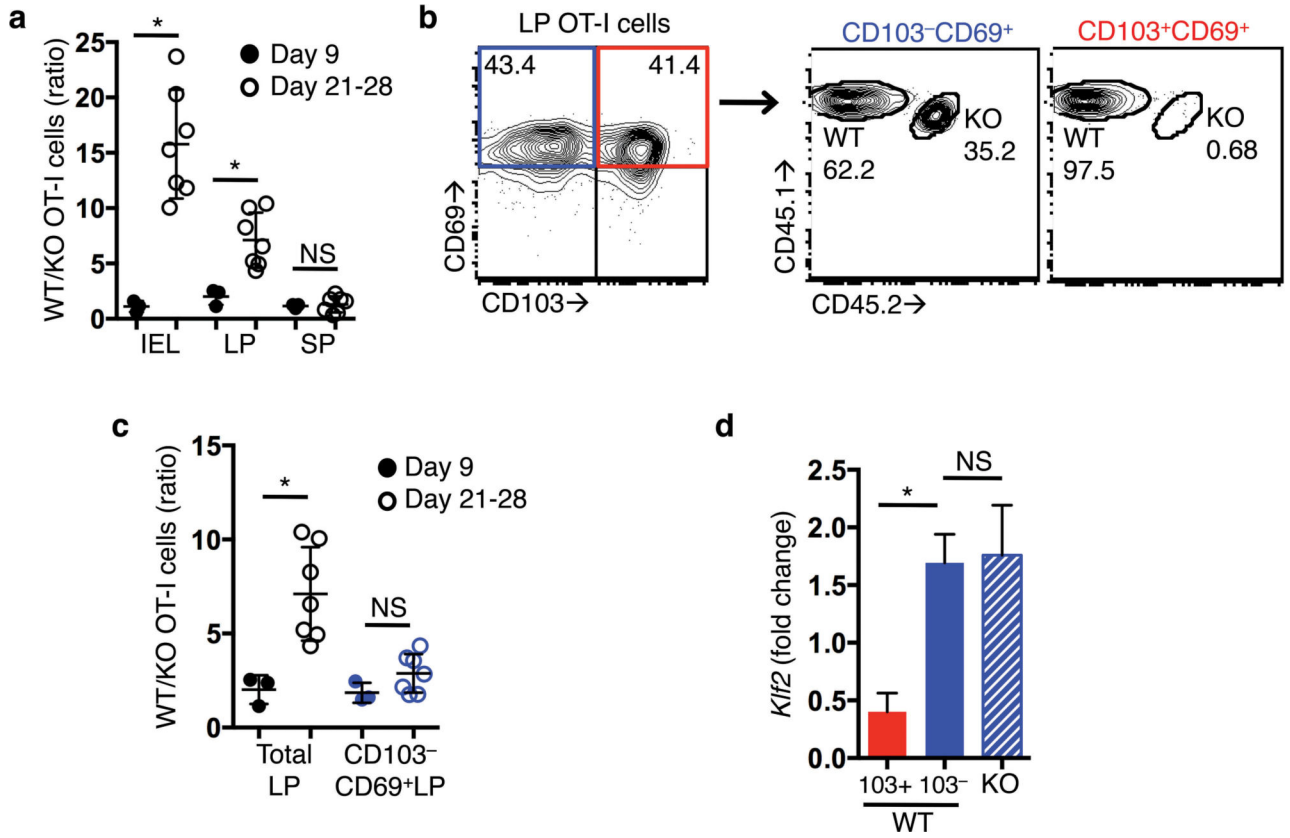


**Figure 3.** TGF- $\beta$  signaling is not required for development of the CD103<sup>-</sup> CD8 LP T<sub>RM</sub> cell population.  $5 \times 10^3$  each CD45.1 WT (*Tgfr2*<sup>fl/fl</sup>) and CD45.1/2 *Tgfr2* KO (*Tgfr2*<sup>fl/fl</sup>  $\times$  *dLck-Cre*) OT-I cells were transferred into C57BL/6 mice and one day later mice were infected with Yptb-OVA. OT-I cells were analyzed on the indicated days post infection. **(a)** Ratio of WT to *Tgfr2* KO OT-I cells in various tissues at the indicated days post infection. Data points represent individual mice. **(b-c)** CD103 and CD69 expression on OT-I cells from the LP. Ratio of WT/KO OT-I cells in the CD103<sup>+</sup>CD69<sup>+</sup> and CD103<sup>-</sup> CD69<sup>+</sup> LP populations. Data points in **(c)** represent individual mice. **(d)** The indicated OT-I populations were sorted from the LP at greater than 21 days post infection. RNA was isolated and *Klf2* expression was determined using qRT-PCR and levels were normalized to *Actb* expression. The *Klf2* mRNA levels for WT OT-I splenocytes were set to 1. **(a-d)** Data pooled from two independent experiments with 3-4 mice/group. \* $p < 0.001$  (unpaired **(a,c)** or paired *t*-test **(d)**).

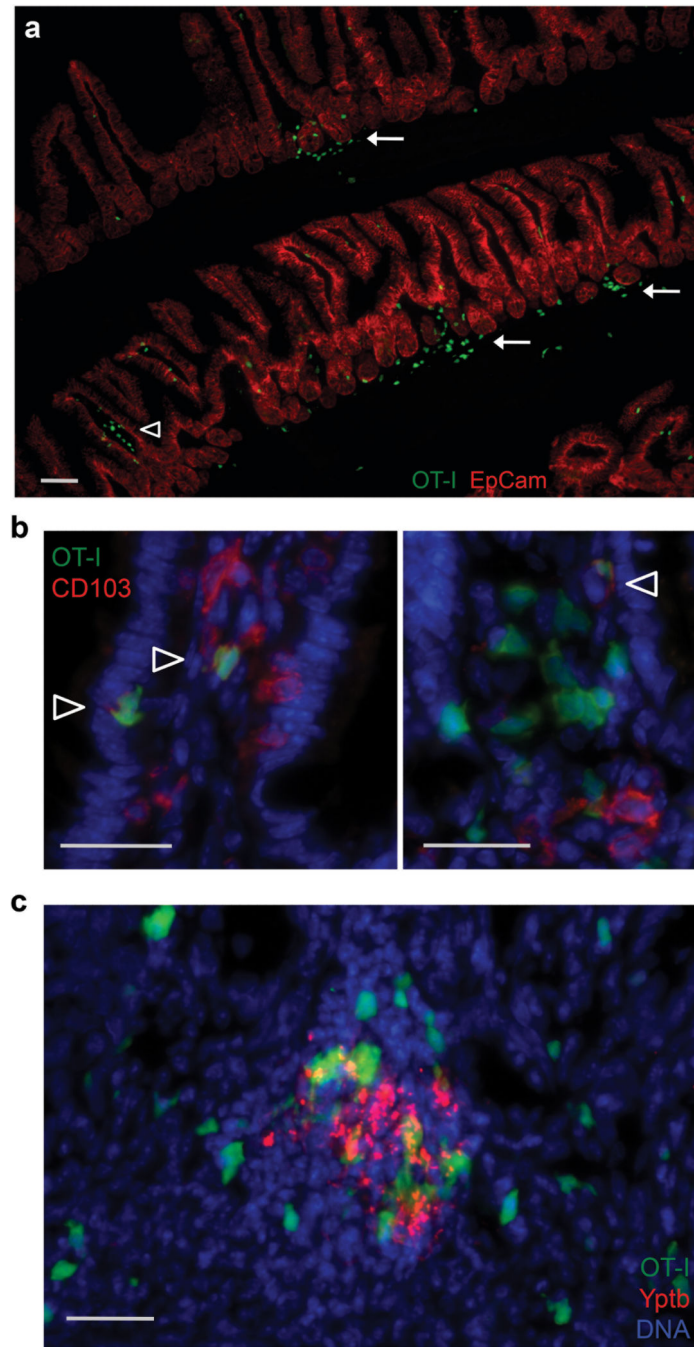


**Figure 4.** Yptb-OVA infection stimulates formation of CD103<sup>-</sup> CD8 T cell clusters in the LP. C57BL/6 mice received  $10^4$  GFP OT-I T cells and were orally infected with Yptb-OVA the following day. The terminal ileum was isolated at 9 days post infection and tissue sections were analyzed by immunohistochemistry. **(a)** Distribution of OT-I T cells (green) in the ileum. Arrows indicate LP clusters near the crypts and open arrowheads indicate those in the upper part of the villi. Epithelial cells are stained with anti-EpCam antibody (red). Scale bar equals 100  $\mu$ m. Representative image from 5 mice. **(b)** Tissue sections were stained with

anti-CD103 antibody (red) to determine expression on OT-I T cells (green). Nuclei are stained with DAPI (blue). Open arrowheads indicate CD103<sup>+</sup> OT-I T cells. Images of villous (left) and clustered (right) OT-I T cells. **(c)** OT-I clusters form around areas of Yptb-OVA infection (anti-Yptb-red, OT-I-green, nuclei-blue). **(b-c)** Representative images from 3 mice. Scale bars equal 25  $\mu$ m.

Author Manuscript

Author Manuscript

Author Manuscript

Author Manuscript

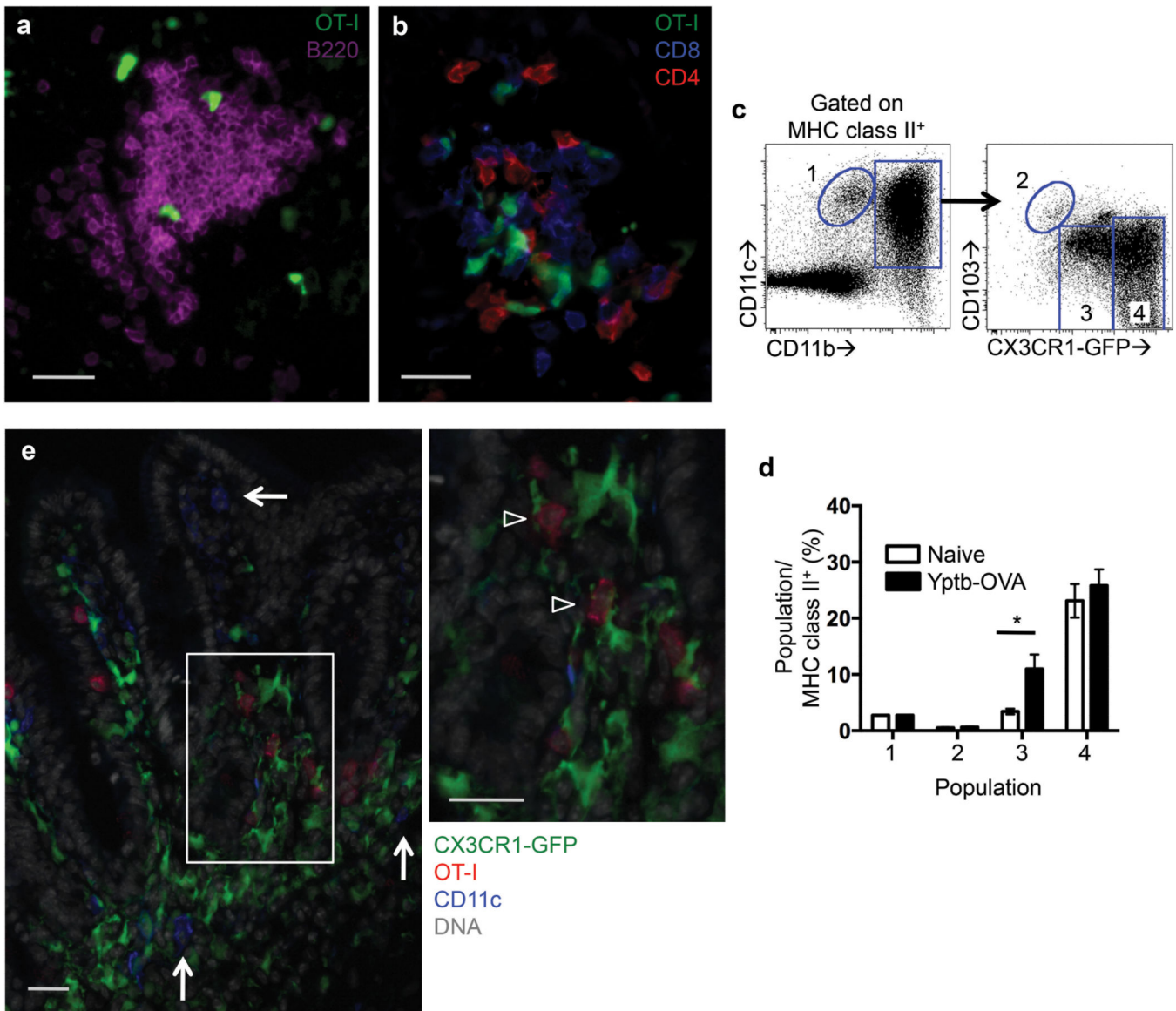


**Figure 5.**

Yptb-OVA induced clusters contain T cells and CX3CR1<sup>+</sup> macrophages and/or DCs but not B cells. OT-I cells were transferred into C57BL/6 (**a,b**) or *Cx3cr1<sup>gfp/+</sup>* (CX3CR1-GFP) (**e**) mice and one day later mice were orally infected with Yptb-OVA. On day 9 post infection, the distribution of OT-I cells and other immune cells in the ileum was analyzed by immunohistochemistry. OT-I (green) localization near (**a**) B220<sup>+</sup> cells (purple) and (**b**) CD4 and CD8 T cells (red and blue, respectively). Scale bars equal 25 μm. Representative data from 3-5 mice (**a,b**). (**c,d**) CX3CR1-GFP mice were infected with Yptb-OVA and on day 7 post infection LP cells were isolated and compared to naive controls. (**e**) Flow cytometry analysis of populations by expression of MHC class II, CD11c, CD11b, CD103, and CX3CR1-GFP. (**d**) Cell populations are graphed as a percent of total MHC class II<sup>+</sup> LP cells; data are means and SDs pooled from 2 experiments with 4-7 mice/group. \**p*<0.05

(unpaired *t*-test). (e) CD90.1 OT-I (red) localization near CD11c (blue) and CX3CR1-GFP expressing cells. Scale bars equal 25  $\mu$ m. Representative data from 3 mice.

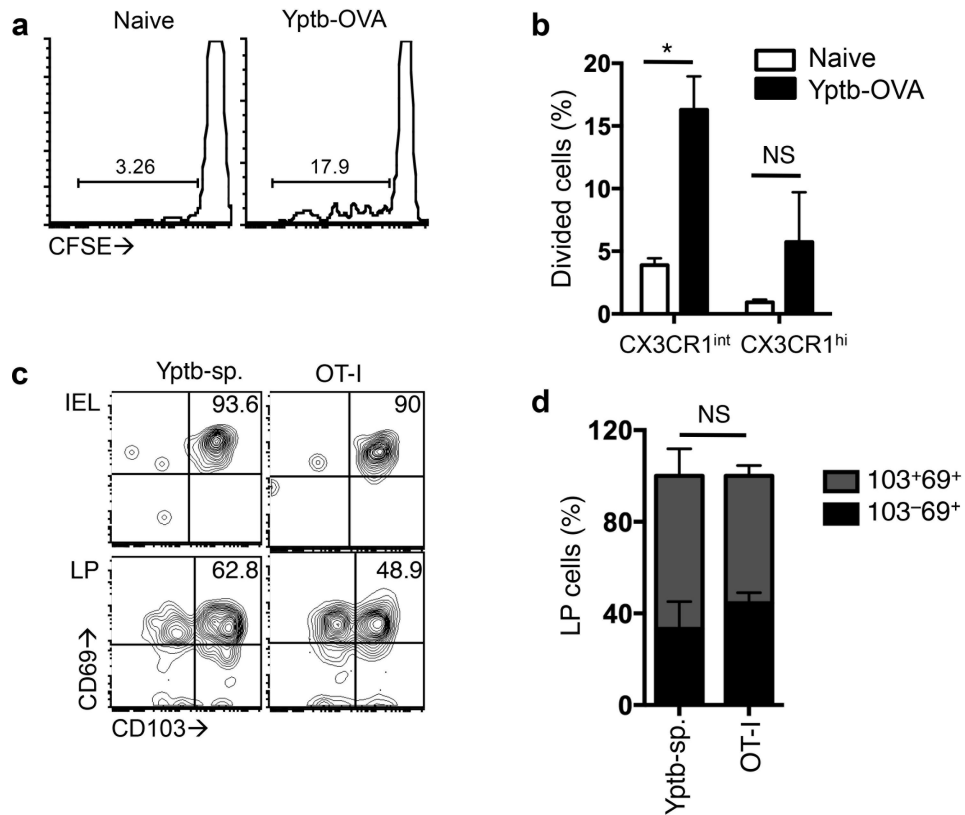
Author Manuscript

Author Manuscript

Author Manuscript

Author Manuscript



**Figure 6.**

CX3CR1-expressing macrophage and/or DC populations present Yptb-OVA antigens, but antigenic stimulation does not downregulate CD103 expression on intestinal T<sub>RM</sub> cells. (a,b) LP macrophage and/or DC populations were sorted from naive and day 6 Yptb-OVA infected *Cx3cr1<sup>gfp/+</sup>* (CX3CR1-GFP) mice as in Fig. 5d. Sorted populations were mixed with CFSE-labeled memory CD8 T cells from Yptb-OVA immune mice and incubated for 3 days. A representative plot indicating the percentage CD8 T cells that underwent division in response to CX3CR1<sup>int</sup> antigen-presenting cells (a) and means and SDs from 3 biological replicates (b). \**p*<0.001 (unpaired *t*-test). (c,d) On day 6 after Yptb-OVA infection, CD8 T cells from the MLN and spleen were transferred into mice infected 6 days earlier with Yptb-NEG. Nine days after transfer, IEL or LP cells were isolated and CD103 expression on Yptb antigen-specific (Yptb-sp.) and antigen non-specific (OT-I) CD8 cells was determined (c) and LP data was quantified in (d) and represents the percent CD103<sup>+</sup> and CD103<sup>-</sup> cells within the CD69<sup>+</sup> population. Data are means and SDs pooled 2 independent experiments with 4 mice total; analyzed using paired Student's *t*-test.

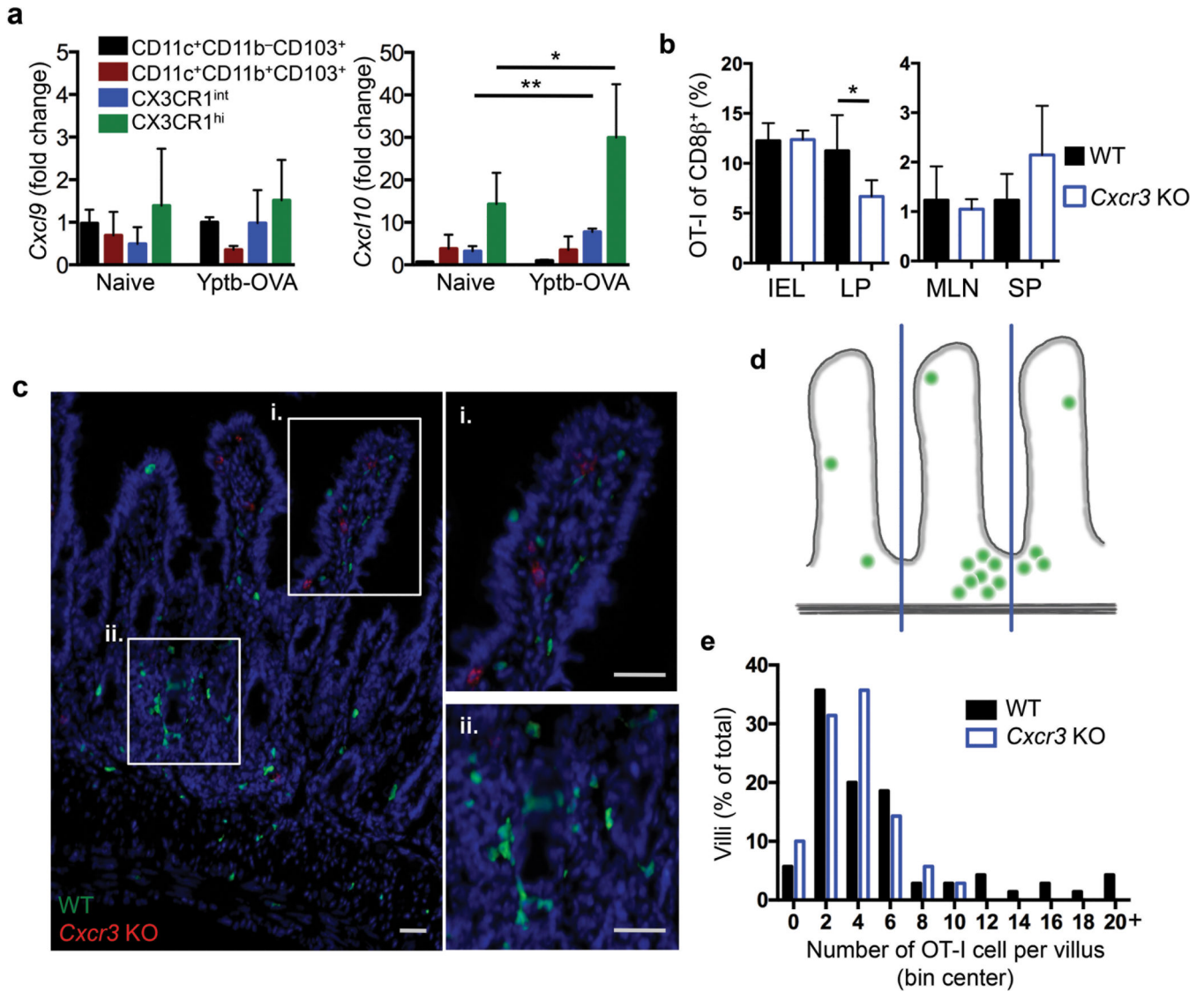


**Figure 7.** *Cxcr3* KO T cells enter the intestine, but fail to localize to areas of inflammation. (a) Intestinal macrophage and/or DC populations were sorted as in Fig. 5d, RNA was isolated and expression of *Cxcl9* and *Cxcl10* was determined by qRT-PCR. Chemokine expression normalized to expression of *Actb*. Data are means and SDs from 2 biological replicates. \*  $p < 0.01$ , \*\*  $p < 0.001$  compared to the same population from naive mice (unpaired *t*-test). (b-e)  $5 \times 10^3$  each GFP wild-type and CD90.1 *Cxcr3* KO OT-I cells were transferred into C57BL/6 mice and one day later mice were infected with Yptb-OVA. OT-I cells were analyzed on day 9 post infection. (b) Wild-type and *Cxcr3* KO OT-I cells in tissues expressed as a percent of total CD8 $\beta^+$  T cells. Data are means and SDs from an individual experiment with 4 mice; representative of 3 experiments. \*  $p < 0.01$  (paired *t*-test). (c) Distribution of wild-type (green) and *Cxcr3* KO (red) OT-I T cells in the ileum. Nuclei are stained with DAPI (blue). Boxes indicate an area of uniform OT-I distribution (i) and an OT-I cluster (ii), with expanded images of the highlighted areas. Scale bars equal 25 $\mu$ m. Images are representative

of 5 mice. **(d)** The number of OT-I cells per villus in the ileum was determined as shown. **(e)** Quantification of the number of wild-type and *Cxcr3* KO OT-I T cells per villus. Distribution of wild-type and *Cxcr3* KO cells are significantly different,  $p < 0.01$  (Chi-squared test). Data are from a single experiment with 2 mice and representative of 3 experiments.

Author Manuscript

Author Manuscript

Author Manuscript

Author Manuscript

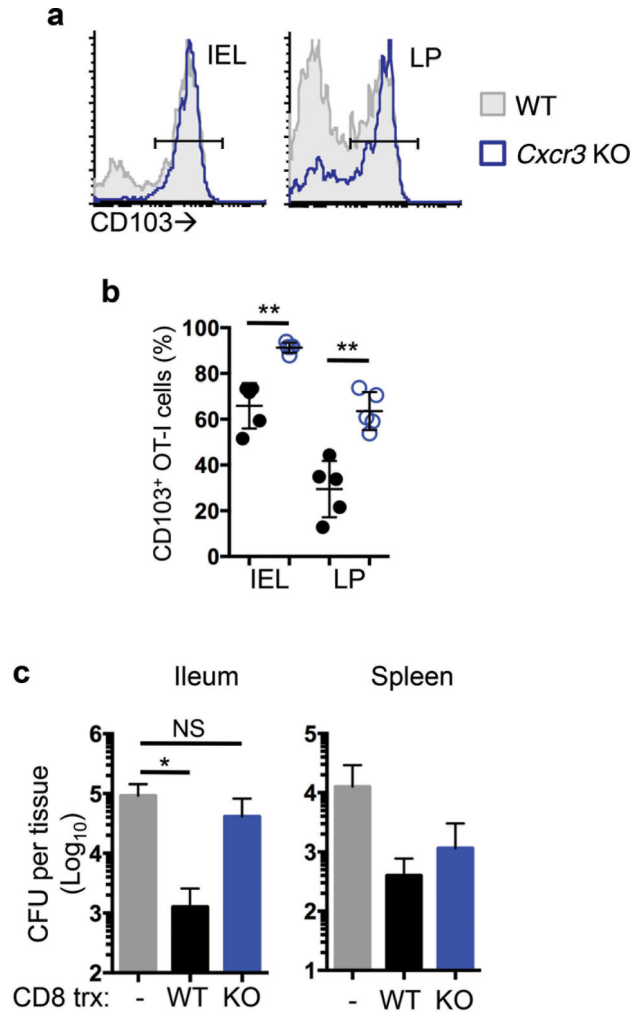


**Figure 8.** CXCR3-mediated localization affects expression of CD103 on intestinal T<sub>RM</sub> CD8 cells and protection.  $5 \times 10^3$  GFP wild-type and CD90.1 *Cxcr3* KO OT-I cells were transferred into C57BL/6 mice and one day later mice were infected with Yptb-OVA. OT-I cells were analyzed on day 9 post infection. **(a,b)** CD103 expression on OT-I T cells in the IEL and LP compartments. Plots are of individual mice and representative of 3 independent experiments **(a)**. **(b)** Data are means and SDs from a single experiment; data points represent individual mice. Representative of three independent experiments. \* $p < 0.01$ , \*\* $p < 0.001$  (paired *t*-test). **(c)** Recipient mice were T cell depleted and infected with Yptb-OVA. Two days later mice received wild-type CD4 T cells and  $7.5 \times 10^5$  wild-type or *Cxcr3* KO CD8 T cells from day 7 Yptb-OVA donor mice. Three days after T cell transfer, ileum and spleen were isolated, homogenized, and plated on CIN agar and bacterial CFU calculated. Data are means and SDs from a single experiment with 3 mice/group, representative of 2 experiments. \* $p < 0.05$  (unpaired *t*-test).